Fe(III) stabilizing soil organic matter and reducing methane emissions in paddy fields under varying flooding conditions

Zheng Sun, Huabin Li, Jinli Hu, Xian Wu, Ronglin Su, Ling Yan, Xiaolei Sun, Muhammad Shaaban, Yan Wang, Katell Quénéa, et al.

Ecotoxicology and Environmental Safety 259 (2023) 114999

Contents lists available at ScienceDirect

Ecotoxicology and Environmental Safety

journal homepage: www.elsevier.com/locate/ecoenv

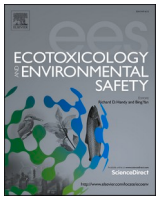

Fe(III) stabilizing soil organic matter and reducing methane emissions in paddy fields under varying flooding conditions

Zheng Sun [a,b,c], Huabin Li [a], Jinli Hu [a], Xian Wu [a], Ronglin Su [a], Ling Yan [a,d], Xiaolei Sun [e], Muhammad Shaaban [f], Yan Wang [a], Katell Quénéa [b], Ronggui Hu [a,*]

[a] Key Laboratory of Arable Land Conservation (Middle and Lower Reaches of the Yangtze River), Ministry of Agriculture, College of Resources and Environment, Huazhong Agricultural University, Wuhan 430070, China
[b] Sorbonne Universités, CNRS, EPHE, UMR 7619 METIS, 4 place Jussieu, 75252 Paris Cedex 05, France
[c] IFP Energies Nouvelles, Geosciences Division, 1 et 4 Avenue de Bois-Préau, 92852 Rueil-Malmaison Cedex, France
[d] Zhengzhou Yuanzhihe Environmental Protection Technology Co., Ltd., Zhengzhou, Henan, China.
[e] Institute of Bio and Geosciences, Agrosphere (IBG-3), Forschungszentrum Jülich GmbH, 52425, Jülich, Germany
[f] College of Agriculture, Henan University of Science and Technology, Luoyang, Henan Province 471003, China

ARTICLE INFO

Edited by G. Liu

Keywords:
Iron redox cycling
Soil organic matter stabilization
Paddy soil
Greenhouse gas emissions
Oxic and anoxic environments

ABSTRACT

The role of iron (Fe) in soil organic matter (SOM) stabilization and decomposition in paddy soils has recently gained attention, but the underlying mechanisms during flooding and drying periods remain elusive. As the depth water layer is maintained in the fallow season, there will be more soluble Fe than during the wet and drainage seasons and the availability of oxygen (O_2) will be different. To assess the influence of soluble Fe on SOM mineralization during flooding, an incubation experiment was designed under oxic and anoxic flooding conditions, with and without Fe(III) addition. The results showed that Fe(III) addition significantly ($p < 0.05$) decreased SOM mineralization by 14.4 % under oxic flooding conditions over 16 days. Under anoxic flooding incubation, Fe(III) addition significantly ($p < 0.05$) decreased 10.8 % SOM decomposition, mainly by 43.6 % methane (CH_4) emission, while no difference in carbon dioxide (CO_2) emission was noticed. These findings suggest that implementing appropriate water management strategies in paddy soils, considering the roles of Fe under both oxic and anoxic flooding conditions, can contribute to SOM preservation and mitigation of CH_4 emissions.

1. Introduction

Rice paddy soils contain 18 Pg carbon worldwide and account for 14 % of the total soil organic carbon (SOC) pool in croplands, and rice paddy soils have great potential to stabilize more carbon in global scale (Liu et al., 2021). The rice paddy ecosystem is an intermediate wet ecosystem between terrestrial and aquatic ecosystems (Khan et al., 2013; Peng et al., 2015; Xu et al., 2019). Various water irrigation modes are practiced in south China, including traditional irrigation, intermittent irrigation, and controlled irrigation (Hou et al., 2012). The alternating flooding and drainage conditions affect the O_2 concentration and create changing aerobic and anaerobic conditions. Such aerobic and anaerobic cycling leads to temporal variations in soil O_2 concentrations and a high content of Fe as a suspended or dissolved form in the water layer in paddy soil (Cleveland et al., 2010; Li and Horikawa, 1997), which induce high variation in carbon mineralization (Ginn et al., 2017; McNicol and Silver, 2015; Schädel et al., 2016).

Fe-carbon association is one of most important mechanisms in regulation SOC storage and persistence not only in paddy soil but also in various ecosystems (Wagai and Mayer, 2007). The Fe(III)-Fe(II) redox cycle has been demonstrated to play a vital role in organic carbon mineralization and stabilization in subtropical paddy soil in numerous studies (Li et al., 2012; Thompson et al., 2006; Thompson et al., 2011). The redox condition mediated by the fluctuation of soil O_2 concentration by water fluctuation usually regulates SOM mineralization and stabilization (Li et al., 2012). The Fe(III)-Fe(II) cycle in paddy soil is driven both by abiotic chemical reactions and microbially mediated processes (Melton et al., 2014). Fe(II) can be easily oxidized by O_2 or NO_3^- via biological or chemical reactions (Melton et al., 2014; Weber et al., 2006). Fe(II) oxidation stimulates the decomposition of organic matter

* Correspondence to: College of Resources and Environment, Wuhan 430070, China.
E-mail addresses: zheng.sun@sorbonne-universite.fr, sunzhengasuka@gmail.com (Z. Sun), rghu@mail.hzau.edu.cn (R. Hu).

https://doi.org/10.1016/j.ecoenv.2023.114999
Received 10 February 2023; Received in revised form 5 May 2023; Accepted 8 May 2023
Available online 11 May 2023

by (a) organic matter oxidation, likely driven by reactive oxygen species, and (b) increases dissolved organic carbon availability, likely driven by acidification (Hall and Silver, 2013). In contrast, the oxidation of Fe(II) to Fe(III) limits the accessibility of organic matter to microbes, enzymes, and oxygen to protect SOM via sorption and coprecipitation (Hall et al., 2016; Huang et al., 2019; Lützow et al., 2006; Riedel et al., 2013; Spohn and Giani, 2010). Fe(II) oxidation can suppress dissolved organic matter decomposition under oxic condition (Chen et al., 2020).

The forms of iron present in soil play different roles in SOM preservation and degradation. Fe(III) oxide is crucial for protecting SOM via sorption, adsorption, or cover (Kaiser and Zech, 2000; Lalonde et al., 2012b; Riedel et al., 2013; Wang et al., 2019; Zhao et al., 2016). However, Fe(III) serves as an electron acceptor in an anoxic environment for microbial respiration, leading to Fe(III) oxide reduction and dissolution (Dubinsky et al., 2010). Consequent desorption and release of organic matter protected by organo-mineral interactions are caused by reduction and dissolution (Hall and Huang, 2017; Pan et al., 2016; Pasakarnis et al., 2015; Zhao et al., 2017). SOM degradation is tightly coupled with Fe(III) reduction in an anaerobic environment. The enzymatic reduction of Fe(III) to Fe(II) can supply energy for microorganisms (Fortin and Langley, 2005; Weber et al., 2006). Fe-reducing bacteria (FeRB), such as *Geobacter* spp. or *Shewanella* spp., can reduce Fe(III) by decomposing SOM and can transfer electrons from SOM to Fe(II) in anaerobic environments both directly and indirectly (Fortin and Langley, 2005; Melton et al., 2014; Neubauer et al., 2005; Weber et al., 2006). The concentration of soluble Fe in paddy soil can vary greatly depending on a number of factors, including the soil type, climate, land use, and management practices. Under flooded conditions, which are typical in paddy soils, the concentration of soluble Fe can be quite low due to the reducing conditions that prevail in the soil (Fageria et al., 2008). In general, high levels of soluble Fe can increase the decomposition of organic matter and reduce SOC levels, while low levels of soluble Fe can have the opposite effect (Kwan and Voelker, 2002). High levels of soluble Fe can stimulate the growth and activity of certain soil microorganisms, leading to increased decomposition of organic matter and reduced SOC levels (Chen et al., 2020). In addition, the concentration of soluble Fe can also be influenced by the presence of other nutrients, such as nitrogen and phosphorus, which can impact the decomposition of organic matter and the formation of SOC (Khan et al., 2019; Yi et al., 2022). In conclusion, the concentration of soluble Fe in soil can have a significant impact on SOC levels, and managing Fe levels in soil can play a role in maintaining SOC and soil fertility.

Numerous studies have documented the effect of O_2 concentration on Fe redox coupling with SOM mineralization (Coby et al., 2011; Mejia et al., 2016; Sun et al., 2019). However, few studies have focused on the influence of suspended and soluble Fe(III) on SOM mineralization under aerobic and anaerobic conditions. The soluble Fe (III) oxidizes to flow mainly in amorphous in low PO_2 show potential impact on SOC protection (ThomasArrigo et al., 2022). To determine the effects of Fe(III) addition on SOC mineralization under oxic and anoxic environments, we designed an incubation experiment to compare SOM decomposition with classic paddy soil by Fe(III) addition under oxic and anoxic conditions. Therefore, evaluating the different roles of Fe in SOM mineralization and stabilization under oxic and anoxic conditions is essential for maintaining SOM during flooding and drying cycles in paddy soil. The research hypotheses are following two points:

a) Fe(III) addition under oxic flooding conditions will decrease SOM mineralization rates, as the increased Fe(III) levels may limit the accessibility of organic matter to microbes and oxygen, thereby enhancing SOM stabilization.
b) Fe(III) addition under anoxic flooding conditions will suppress CH_4 emission by serving as an alternative electron acceptor for microbial respiration, without significantly affecting the overall SOM decomposition rates.

2. Materials and methods

2.1. Site description and treatments

Soil samples were collected from Xiangyin County, Yueyang City, Hunan Province (N 28.71°, E 112.92°). The soil is classified as ultisol according to the USDA (Sun et al., 2019). Soil samples were collected at a depth of 0–20 cm in the fallow season. Soil samples were air-dried at room temperature after roots, plant residues, and stones were removed. Air-dried soil samples were crumbled and sieved (2 mm) before use in experiments. The physical and chemical properties of the tested soil samples are shown in Table 1.

2.2. Soil incubation experiment

In our experiments, the presence or absence of iron addition and the presence or absence of oxygen during the incubation are two factors studied in this experiment. The Fe(III) addition rate ($FeCl_3$, at 5 mg kg^{-1}) corresponded to the soluble Fe content in this paddy soil water profile when we collect the soil samples, which is close to the maximum Fe(III) solubility at neutral pH (Guelke et al., 2010; Kraemer, 2004). Each treatment was applied in triplicate and finally the four treatments are set as follows:

- Oxic: Flooding soil incubated in a 21 % O_2 atmosphere.
- Oxic + Fe(III): Flooding soil incubated in a 21 % O_2 atmosphere and supplied with $FeCl_3$ solution at 5 mg kg^{-1}.
- Anoxic: Flooding soil incubated in a 100 % N_2 atmosphere.
- Anoxic + Fe(III): Flooding soil incubated in a 100 % N_2 atmosphere and supplied with $FeCl_3$ solution at 5 mg kg^{-1}.

The soil was preincubated at 25 °C with 70 % water-filled-pore space (WFPS) moisture for two weeks in a dark incubator (HP-400S Ruihua, Wuhan, China) to create a stable soil environment. After the soil became equilibration, 15 g of dry soil was placed in 72 glass bottles (6 sampling times × 4 treatments × 3 replicates) of volume 150 ml. The treatments without Fe(III) addition were adjusted to flooding conditions (dry soil/water; 1:2 w/v) by adding ultrapure water, and the treatments with Fe (III) addition were adjusted to flooding conditions by adding $FeCl_3$ solution (5 mg kg^{-1}) (dry soil/water; 1:2 w/v). The anoxic treatments were capped with butyl rubber stoppers with plastic seals, and the air inside was replaced with pure N_2 gas. The oxic treatments were also capped with butyl rubber stoppers with plastic seals, and the air inside was replaced with O_2-N_2 mixed gas (21 % O_2 and 79 % N_2). All samples were incubated in a 25 °C dark incubator for 16 days.

After 1, 3, 5, 7, 10, and 16 days, soil sub-samples were collected to measure oxidation–reduction potential (ORP), dissolved oxygen (DO), ammonium, nitrate, Fe(II), and Fe(III) content, while headspace gas samples to quantify CO_2 and CH_4. On each sampling day, we withdrew the headspace gas samples by syringes. Then, we mixed content in each glass bottle using a vortex shaker and obtained the homogeneous slurry to determine the ammonium, nitrate, Fe(II), and Fe(III) concentrations. The experiments for anoxic treatments were carried out in an anaerobic chamber.

2.3. Analytical methods

Soil texture was determined by the pipette method (Kettler et al., 2001). The content of soil total organic carbon (C) and nitrogen (N) were determined by an elemental analyzer (Vario MAX CN, Elementar, Germany). The total Fe was dissolved in a concentrated acid mixture of $HClO_4$-HF after calcination of SOM at 450 °C (Huang et al., 2018). The extracts were measured using atomic absorption spectroscopy (AA240FS; Agilent, Santa Clara, CA, USA).

To avoid disturbing the samples and soil contacting the gas sphere, which could induce rapid oxidation in the soil, we used two

Table 1
Physical and chemical properties of the soil used in the experiment.

Site	pH	Total C (g kg-1)	Total N (g kg-1)	Total Fe (g kg-1)	Fed (g kg-1)	Feo (g kg-1)	Fep (g kg-1)	Fe-HCl (g kg-1)	Texture Silt (%)	Clay (%)	Sand (%)
Yueyang	5.27 ± 0.00	19.50 ± 0.04	2.17 ± 0.00	24.53 ± 0.41	19.98 ± 0.26	4.15 ± 0.03	0.71 ± 0.01	2.64 ± 0.04	60.1 ± 1.92	34.5 ± 1.28	5.4 ± 0.82

Standard errors (n = 3 replicate samples) are shown in parentheses.
Contents of iron oxide (Fed) - iron extracted by dithionite-citrate-bicarbonate (DCB); amorphous iron (Feo) - iron extracted by acid ammonium oxalate (AAO); complexed iron (Fep) - iron extracted by sodium pyrophosphate; active iron (Fe-HCl) - iron extracted by hydrochloric acid.

microelectrodes to measure DO and ORP. The DO concentrations were measured with a Clark-type microelectrode (Ox100, Unisense, Aarhus, Denmark), and ORP values were measured with a Clark-type microelectrode (Rd100, Unisense, Aarhus, Denmark) (Bussmann et al., 2006; Hansen et al., 2014).

The bioavailable Fe(II) and Fe(III) were extracted in an anaerobic chamber with 0.5 mol L^{-1} HCl from the soil slurry (Gault et al., 2011). The extracted Fe(II) was analyzed by the colorimetric method with a UV-Vis spectrometer as described by Tamura et al. (1974). After adding hydroxylamine hydrochloride to the soil extract, the total extracted iron was determined by the same colorimetric method with a UV-Vis spectrometer. The addition of hydroxylamine hydrochloride reduced Fe(III) to Fe(II), making it possible to measure the total iron concentration in the soil extract. The amount of Fe(III) was then calculated as the difference between the total extracted iron and Fe(II) (Tamura et al., 1974; Wang et al., 2016). The dithionite-citrate-bicarbonate (Fe-DCB) method of Holmgren (1967) was used to measure the total Fe-(hydr)oxide soil content, which includes both short-ranged ordered Fe-(hydr)oxides and goethite. The extraction method of Schwertmann (1973) is used to determine the amount of amorphous iron in acidic ammonium oxalate. The Fe content bound with SOM is extracted using sodium pyrophosphate as described by McKeague (1967).

The CO_2 and CH_4 concentrations were analyzed by gas chromatography in the gas samples (Agilent 7890 A, Agilent Technologies Inc., Santa Clara, CA, USA) with a flame ionization detector (FID) (Wang and Wang, 2003).

Ammonium-nitrogen (NH_4^+-N) and nitrate-nitrogen (NO_3^--N) in the fresh slurry were extracted by shaking the soil with 10 % potassium chloride (KCl) for 30 min. Then the extracted residues will be weighed to know their dry mass. The extracted solutions were filtered and stored in a deep freezer (–18 °C) until analysis. Both NH_4^+-N and NO_3^--N contents were measured by a colorimetric method using a UV–Vis spectrometer. NH_4^+-N was measured by the phenol hypochlorite method, and NO_3^--N was measured by the modified Griess-llosvay method (Moorcroft et al., 2001; Scheiner, 1976). The NO_3^--N contents of the soil samples were below the detection limit and were neglected.

2.4. Data calculations and model analysis

Carbon decomposition (*Dec C*) was estimated from CO_2 emission and CH_4 emission. N mineralization (*Min N*) was estimated taking the difference between the initial and final day NH_4^+-N content.

GraphPad Prism 8.0 (GraphPad, La Jolla, CA) was used to generate the C decomposition ($CO_2 + CH_4$) and N mineralization time curves by the first-order reaction model. The C decomposition potential (C_0) was estimated as described by the following equation (Ameloot et al., 2014):

$$Dec \quad C = C_0(1 - \exp(-K_C \times t))$$

where C_0 is the C decomposition potential (g C kg^{-1}), K_C is the C decomposition rate constant (d^{-1}), and t is the incubation time (d).

The N mineralization potential (N_0) was determined using the following equation (Cheng et al., 2016):

$$Min \quad N = N_0(1 - \exp(-K_N \times t))$$

where N_0 is the N mineralization potential (g N kg^{-1}), K_N is the N mineralization rate constant (d^{-1}), and t is the incubation time (d).

One-way analysis of variance (ANOVA) was used to compare the differences between treatments. Three-way repeated-measures ANOVA was used to explore the impact of the factors. Multiple linear regression and linear regression were built between ORP and DO and Fe (III) content. Differences were considered significant at $p < 0.05$. Statistical analyses were conducted using the SPSS software package (SPSS 24.0 for Windows, Chicago, Illinois, USA). The figures were plotted using GraphPad Prism software package (GraphPad Prism 8.0.0 for Windows, San Diego, California USA).

3. Results

3.1. The DO and ORP in soil

During incubation, DO concentrations decreased from 9.0 mg L^{-1} to close to 0 mg L^{-1} in the treatments with O_2 present (Fig. 1a). The rate of the DO concentration decrease was more rapid in the treatment of oxic than in oxic + Fe(III). The DO in oxic treatment decreased to 0 mg L^{-1} in 3 days, whereas it took 7 days to reach approximately 0 mg L^{-1} in oxic + Fe(III) treatment. The DO concentration was consumed much faster in oxic treatment than in oxic + Fe(III) treatment and maintained at 0 mg L^{-1}, which shows that Fe(III) addition significantly ($p < 0.01$) decreased the rate of DO depletion under aerobic conditions (Fig. 1a). Both the presence of O_2 and Fe(III) addition significantly ($p < 0.01$) retarded the DO depletion rate in the samples (Supplementary Table 1).

The ORP decreased from 347.7 mV to a low plateau after 5 days in oxic treatment and 7 days in oxic + Fe(III) treatment (Fig. 1b). Fe(III) addition suppressed the rate of the ORP decrease ($p < 0.01$, Fig. 1b). The ORP in oxic and oxic + Fe(III) treatments decreased from 347.7 mV to 6.7 mV and 98.9 mV, respectively. The different trends of ORP show that the addition of Fe(III) promoted the ORP plateau under aerobic flooded incubation ($p < 0.01$). In anoxic and anoxic + Fe(III) treatments, Fe(III) addition initially (0–7 days) slowed the rate of the ORP decrease. After seven days, the ORP in anoxic and anoxic + Fe(III) treatments decreased from 347.7 mv to −91.5 mv, which indicates that the addition of Fe(III) resulted in a short-duration increase in ORP during anaerobic flooded incubation. The presence of Fe(III) addition significantly ($p < 0.01$) promoted the full time (0–16 days) ORP in oxic flooding treatment and temporally (0–7 days) ORP in anoxic flooding treatments (Supplementary Table 1).

3.2. The Fe(II) and Fe(III) dynamics during the incubation

Approximately 70 % of the Fe-HCl in the soil was presented as Fe(III), and 30 % of the Fe-HCl was present as Fe(II) as the incubation started (Fig. 2). In aerobic flooded incubation, Fe(II) reached maximum values of 2121.7 and 1822.3 mg kg^{-1} on day 7 in the treatment of oxic and oxic + Fe(III), respectively (Fig. 2). Subsequently, the concentrations of Fe (II) slowly decreased until the end of the incubation. In anaerobic flooded incubation, Fe(III) was gradually reduced to Fe(II) during the incubation in both anaerobic treatments. All Fe(III) was reduced to Fe (II) after 5 and 10 days in the treatment of anoxic and anoxic + Fe(III). However, the Fe(III) reduction rate was slowed by Fe(III) addition in the

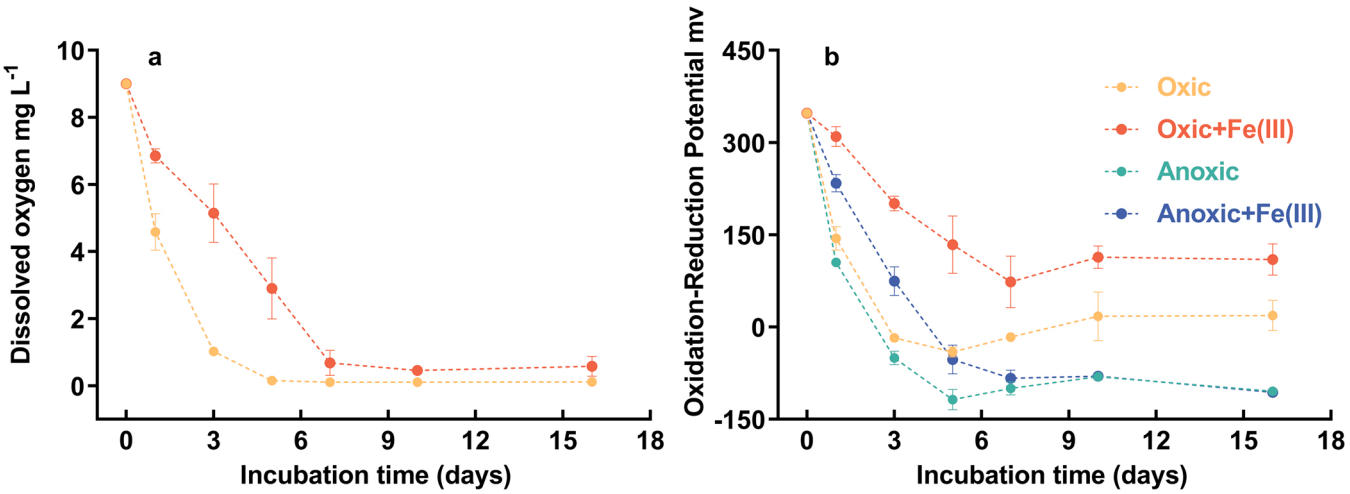

Fig. 1. Evolution of dissolved oxygen contents (a) in oxic treatments and oxidation-reduction potential value (b) in all treatments during the incubation. The values represent the mean of three replicates, and the error bars represent standard errors.

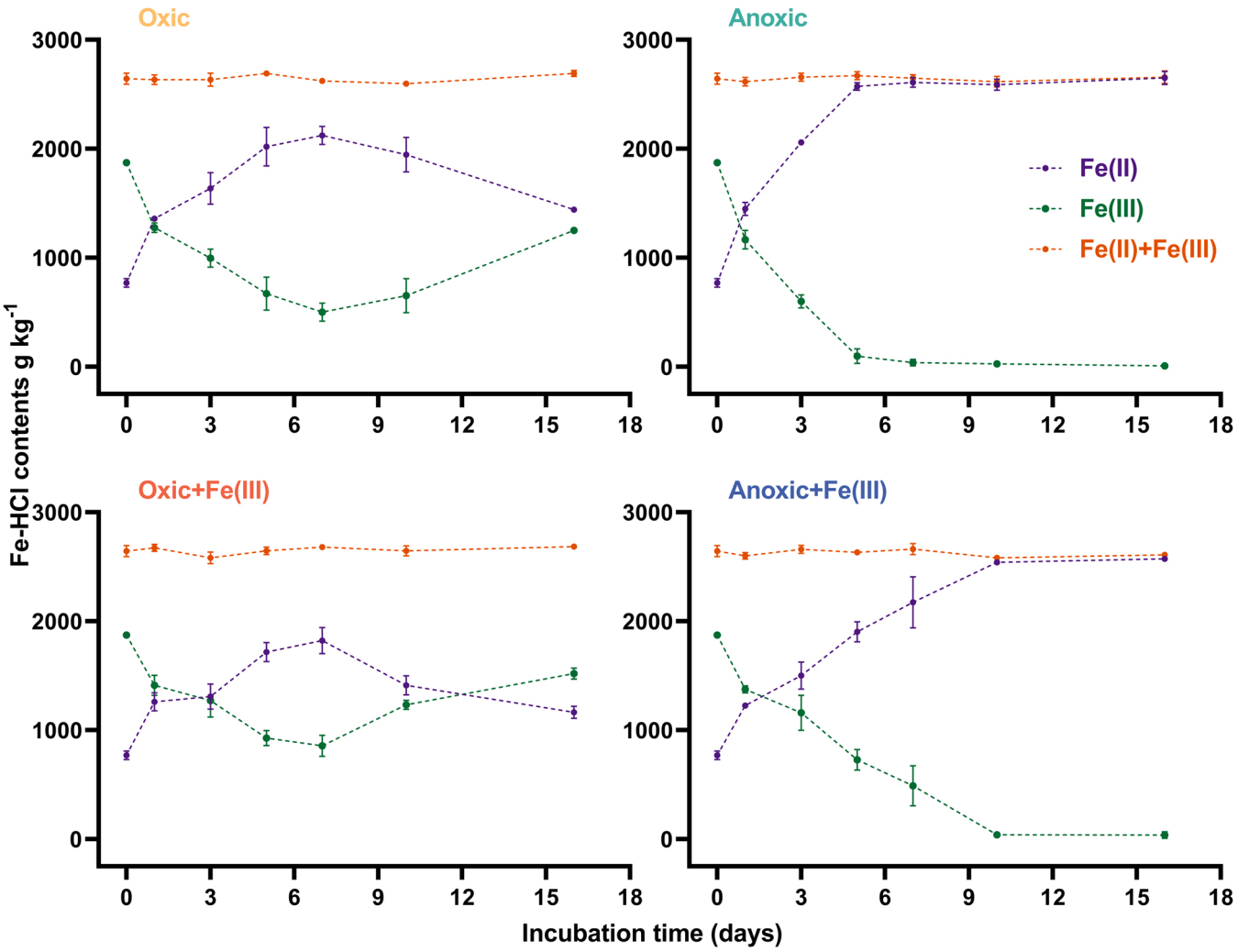

Fig. 2. The contents of Fe (II) and Fe (III) in the soils extracted by 0.5 mol L^{-1} HCl during the incubation in all treatments.

anaerobic treatments. In aerobic treatments, Fe(III) addition significantly decreased the concentration of Fe(II) ($p < 0.01$, Supplementary Table 1).

3.3. Soil CO_2 and CH_4 emission

CO_2 emission showed an exponential increase that followed a first-order reaction model in all treatments (Fig. 3a). In the flooding

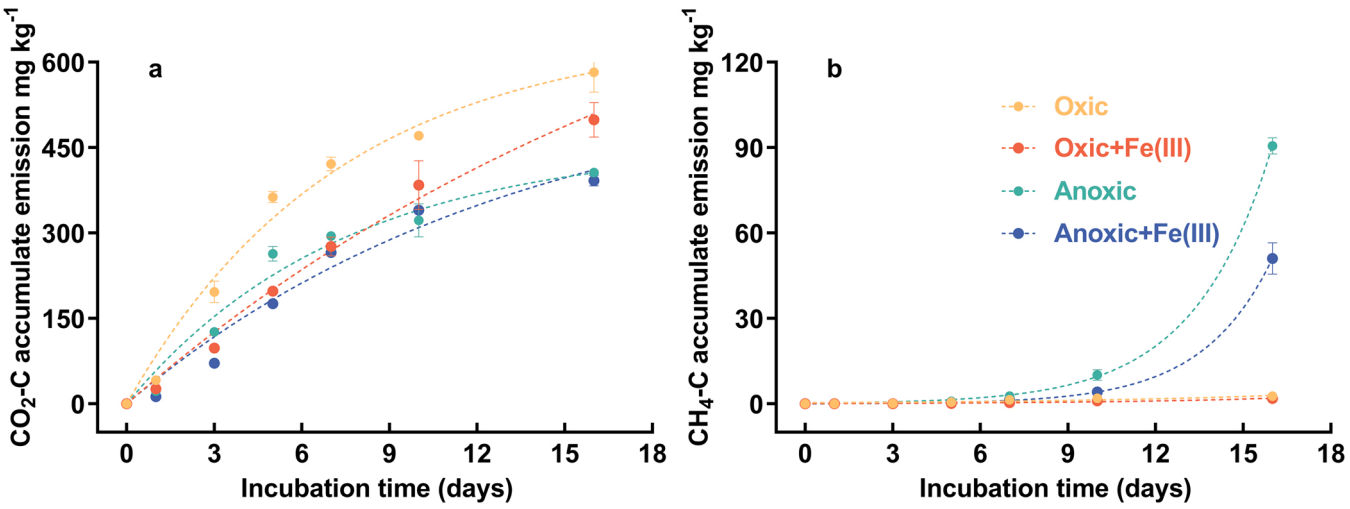

Fig. 3. CO_2 production (a) and CH_4 productions (b) from the soils in all treatments during the incubation. The CO_2 production was modeled by [C = C_0 × (1-exp (-k × t)] and CH_4 production was modeled by [C = a + b × exp (c × t)].

treatments, more CO_2 was produced than in the anaerobic flooding treatments. The average CO_2 emission from the four treatments after 16 days amounted to 582.4, 498.8, 406.1, and 391.9 mg C kg^{-1} soil for the treatment of oxic, oxic + Fe(III), anoxic, and anoxic + Fe(III), respectively. The CO_2 emission of oxic treatment was continuously higher than that of oxic + Fe(III) treatment, while anoxic treatment was higher than anoxic + Fe(III) treatment only in the first five days of the incubation. The presence of O_2 significantly increased CO_2 emission ($p < 0.01$, Supplementary Table 1). The Fe(III) addition induced a decrease in CO_2 emission in the flooding treatments ($p < 0.01$, Supplementary Table 1).

CH_4 emission showed an exponential increase in anaerobic flooding treatments (Fig. 3b). The average CH_4 emission from the four treatments after 16 days amounted to 2.7, 1.9, 90.6, and 51.1 mg C kg^{-1} soil for the treatments of oxic, oxic + Fe(III), anoxic, and anoxic + Fe(III), respectively. As expected, the flooding treatments produced a very small amount of CH_4. The presence of O_2 sharply decreased CH_4 emission in the soil ($p < 0.01$, Supplementary Table 1). Fe(III) addition in anaerobic flooding environments could also significantly decrease CH_4 emission ($p < 0.01$, Supplementary Table 1) since it retards CH_4 emission.

3.4. Carbon decomposition and nitrogen mineralization potentials

The changes in carbon decomposition and nitrogen mineralization in all treatments followed a first-order reaction model (Fig. 4). However, the parameters C_0 and N_0 and K_C and K_N differed among the four treatments (Table 2). Fe(III) addition significantly increased C_0 but decreased K_C ($p < 0.01$, Supplementary Table 1). Moreover, Fe(III) addition did not affect N_0 but decreased K_N.

4. Discussion

4.1. The influence of Fe(III) addition on SOM stabilization and mineralization

The results of the flooding treatments demonstrate that Fe(III) addition played a pivotal role in SOM stabilization (Fig. 4). According to the first-order model of SOM mineralization (Table 2), Fe(III) addition (oxic + Fe(III)) strongly decreased the C decomposition rate (K_C). The mechanisms of lower SOM mineralization are as follows:

(1) The pH in all treatments are neutral, and abiotic oxidation by oxygen dominates the reaction of Fe(III) crystallization. However, the crystallinity is lower than that under abiotic and biotic oxidation at low O_2 levels (Druschel et al., 2008; Emerson et al., 2010; Mejia et al., 2016). Therefore, the addition of Fe(III) contributes to the formation of fine, weak crystal Fe minerals, which

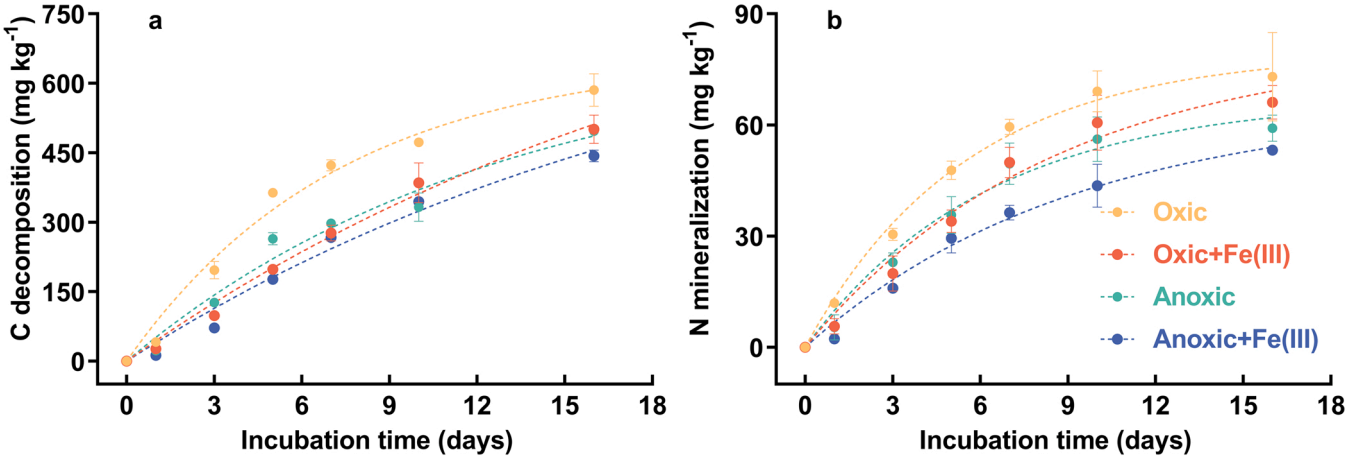

Fig. 4. The carbon (C) decomposition (a) and nitrogen (N) mineralization (b) from the soils in all treatments during the incubation. Both C decomposition and N mineralization were modeled by [C (or N) = C_0 (or N_0) × (1 − exp (−k × t)].

Table 2
The parameters obtained from the incubation experiment at 25 °C after 16 days for measuring the C decomposition potential (C_0) and N mineralization potential (N_0) for the soil samples from treatments. The curves were modeled by first-order model as [C (or N) = C_0 (or N_0) × (1 − exp (−k × t)].

Treatments	C decomposition			N mineralization		
	C_0 mg C kg^{-1}	K_C day^{-1}	R^2	N_0 mg N kg^{-1}	K_N day^{-1}	R^2
Oxic	661.9 ± 49.6b	0.137 ± 0.016a	0.981	81.7 ± 11.2a	0.183 ± 0.057a	0.970
Oxic + Fe(III)	1017.2 ± 246.9a	0.046 ± 0.011c	0.982	82.7 ± 10.5a	0.118 ± 0.023ab	0.961
Anoxic	680.9 ± 14.5b	0.079 ± 0.005b	0.972	67.6 ± 6.0a	0.161 ± 0.026ab	0.959
Anoxic + Fe(III)	855.9 ± 83.9ab	0.048 ± 0.005c	0.978	66.6 ± 3.2a	0.107 ± 0.020b	0.973

KC and KN are the rate constants for the first-order reaction models.
R^2 was the coefficient of determination for each model. All models were fitted significantly at $p < 0.01$. Significant differences between parameters of treatments, indicated by different lowercase letters in the same column, were determined using one-way ANOVA followed by Duncan's multiple range test at $p < 0.05$. The data are shown as the means ± SD (n = 3)

physically protect SOM by preventing contact between SOM and enzymes and O_2 (Keiluweit et al., 2017; Lalonde et al., 2012a; Melton et al., 2014).

(2) Fe(III) polymerization can trap organic matter, especially dissolved organic matter, preventing microbial mineralization (Chen et al., 2014; Riedel et al., 2013; Sodano et al., 2017). The Fe(III) addition might form Fe-P complexes making P less available, perhaps causing a reduction in microbial growth and metabolism (Wen et al., 2019b). Previous research showed that Fe addition could specifically suppress lignin mineralization rather than protect bulk SOM mineralization irrespective of O_2 availability (Hall et al., 2016), which is consistent with our results.

In the anoxic flooding treatments (anoxic and anoxic + Fe(III)), Fe (III) temporally promoted CO_2 emission and suppressed CH_4 emission. Fe(III) rapidly crystallized to short-range Fe minerals that temporarily protect SOM (Wen et al., 2019a). In the late incubation period, Fe(III) was reduced to Fe(II) and lost the ability to protect SOM, so there was no significant difference between the anoxic and anoxic + Fe(III) treatments in CO_2 emission. The SOC decomposition in anoxic treatment was higher than that in anoxic + Fe(III) treatment at the end of the incubation mainly because the CH_4 emission of anoxic treatment was much higher than that of anoxic + Fe(III) treatment, which indicated that Fe (III) addition increased SOC oxidation and suppressed SOC anaerobic degradation. The promotion of ORP by Fe(III) addition was not beneficial for CH_4 emission. The dissimilatory Fe(III) reduction took more time with Fe(III) addition than without Fe(III) addition, thus retarding CH_4 emission. The dissimilatory Fe(III) reduction inhibits methanogenesis through the competition of substrates with methanogens (Hori et al., 2010; Xu et al., 2019), which indicates that Fe(III) temporally suppresses CH_4 emission. In our study, we observed that the addition of Fe(III) did not significantly impact N mineralization. Oxygen was found to be a key factor in influencing the potential for organic N mineralization. Although Fe(III) addition led to a reduction in the organic N mineralization rate (Jansson and Hofmockel, 2020), it is essential to consider that the total SOM mineralization amount may not directly correspond to the presence of added Fe.

In summary, we explored the impact of Fe(III) addition on SOM stabilization and mineralization under oxic and anoxic flooding conditions. It revealed that Fe(III) addition reduced carbon decomposition rates and temporarily affected CO_2 and CH_4 emission under anoxic conditions.

4.2. The influence of O_2 on SOM mineralization

The dynamics of O_2 availability led to the oxidation and reduction of biogeochemical reactions. O_2 is one of the most critical components of the soil redox environment, and it has a direct and rapid effect on microbial activities (McNicol and Silver, 2015). The DO content in soil can be considered a simple depletion process because O_2 diffusion times in water are much lower than those in the air (Kögel-Knabner et al., 2010). Following O_2 depletion, a cascade of alternating electron acceptors is utilized by a diverse set of facultative or obligate anaerobic microorganisms (McNicol and Silver, 2014). Low O_2 availability could slow microbial respiration and activity (Hall and Silver, 2015; McGroddy and Silver, 2000). When O_2 is depleted in soil, Fe undergoes the oxidation and reduction of biogeochemical reactions (Inubushi et al., 2018). Therefore, O_2 accessibility has significant impacts on both redox and SOM mineralization. Furthermore, the O_2 concentration can affect soil redox, which changes the patterns of microbial metabolism and the microbial community. SOM and O_2 could be the direct chemical substrates of SOM decomposition by microbes.

Under flooding incubation, the ORP mainly depended on the DO content (Table 3). Our results indicated that the rate of O_2 depletion was lower in oxic + Fe(III) treatment than in oxic treatment, which demonstrates that Fe(III) addition in a 21 % O_2 atmosphere could reduce DO consumption. At low O_2 contents, Fe(III) is easily crystallized to lepidocrocite, ferrihydrite, or nano goethite (). The high surface area of weak crystalline Fe oxide absorbs dissolved organic matter or coprecipitates with nonparticulate organic matter, which helps to refrain the SOM to be contacted by O_2 and enzymes. According to the soil continuum model (Lehmann and Kleber, 2015), the formation of the mineral surface rapidly adsorbs small biopolymers and monomers, which implies that Fe(III) application protects SOM under aerobic conditions.

There was no oxygen in the soil pores or water layer during anaerobic incubation, and SOM mineralization mostly depended on Fe(III) reduction (Liptzin and Silver, 2015). Our results showed that the ORP mainly depended on the Fe(III) content (Table 3) since O_2 was absent during anaerobic incubation. The dissimilatory reduction process involved Fe(III) reduction by FeRB, which required organic matter as the electron donor (Dubinsky et al., 2010). Therefore, Fe(III) addition limited the contact between organic matter and FeRB, slowing both Fe (III) reduction and SOM mineralization.

In summary, the results examined the influence of O_2 on SOM mineralization and highlights the importance of O_2 availability in affecting microbial activities and redox reactions. Under flooding incubation, Fe(III) addition impacted O_2 consumption and protected SOM under aerobic conditions, while under anaerobic incubation, it limited

Table 3
Multiple linear regression and linear regression between ORP and DO and Fe (III) content.

Treatment	A linear regression model with a partial correlation coefficient	R^2
Oxic	-53.721 + 34.054DO	0.9435
Oxic + Fe(III)	10.335 + 0.0585Fe(III)+ 26.703DO	0.9437
Anoxic	-124.377 + 0.228Fe(III)	0.9409
Anoxic + Fe (III)	-149.023 + 0.241Fe(III)	0.8770

R^2 was the coefficient of determination for each model. All models were fitted significantly at $p < 0.01$.

the contact between organic matter and FeRB, slowing Fe(III) reduction and SOM mineralization.

5. Conclusion

Iron played a crucial role in SOM stabilization and mineralization in paddy soil. In our study, Fe(III) addition showed diverse mechanisms of SOM mineralization occurring in various incubation environments. We found that Fe(III) addition affected SOM mineralization differently under various incubation environments. In line with our first hypothesis, Fe(III) addition during flooding incubation contributed to SOM stabilization by reducing the soil reduction rate and limiting O_2 accessibility. Additionally, in accordance with our second hypothesis, under anaerobic flooding incubation, the presence of soluble Fe(III) increased CO_2 emission but suppressed CH_4 emission. These findings emphasize the importance of soluble Fe in SOM stabilization and mineralization, even when present in low amounts. Future research should investigate the optimization of water management and the effects in long-term of soluble Fe in paddy soils on organic matter stabilization and mineralization in field trials. By investigating these interactions, we can develop improved, environmentally friendly management practices that promote soil health and reduce greenhouse gas emissions.

Funding

This research was supported by the Wuhan Applied Foundational Frontier Project (2020020601012284), the Hubei Technological Innovation Special Fund (2021BCA156), the National Natural Science Foundation of China (41671253 and 41750110485), and Chinese Academy of Sciences President's International Fellowship Initiative (2020PC0066).

CRediT authorship contribution statement

Zheng Sun: Conceptualization, Methodology, Writing - Original Draft, Visualization, Huabin Li: Investigation, Writing - Review & Editing, Supervision, Jinli Hu: Formal analysis, Validation, Writing - Review & Editing, Supervision, Xian Wu: Validation, Writing - Review & Editing, Supervision, Ronglin Su: Investigation, Writing - Review & Editing, Supervision, Ling Yan: Investigation, Writing - Review & Editing, Supervision, Xiaolei Sun: Writing - Review & Editing, Muhammad Shaaban: Data Curation, Writing - Review & Editing, Yan Wang: Writing - Review & Editing, Katell Quénéa: Writing - Review & Editing, Ronggui Hu: Writing - Review & Editing, Supervision, Project administration, Funding acquisition.

Declaration of Competing Interest

The authors declare that they have no known competing financial interests or personal relationships that could have appeared to influence the work reported in this paper.

Data Availability

Data will be made available on request.

Acknowledgments

We thank Dr. Lei Wu and Milan Wang for providing suggestions on the experimental design. We thank senior students of our lab for collecting the soil samples. We also thank to the comments from the reviewers to imrpove the quality of this study.

Ethics declarations

The authors declare no competing interests.

Appendix A. Supporting information

Supplementary data associated with this article can be found in the online version at doi:10.1016/j.ecoenv.2023.114999.

References

Ameloot, N., et al., 2014. C mineralization and microbial activity in four biochar field experiments several years after incorporation. Soil Biol. Biochem. 78, 195–203.
Bussmann, I., et al., 2006. Cultivation of methanotrophic bacteria in opposing gradients of methane and oxygen. FEMS Microbiol. Ecol. 56, 331–344.
Chen, C., et al., 2014. Properties of Fe-organic matter associations via coprecipitation versus adsorption. Environ. Sci. Technol. 48, 13751–13759.
Chen, C., et al., 2020. Iron-mediated organic matter decomposition in humid soils can counteract protection. Nat. Commun. 11, 2255.
Cheng, W.G., et al., 2016. Changes in the soil C and N contents, C decomposition and N mineralization potentials in a rice paddy after long-term application of inorganic fertilizers and organic matter. Soil Sci. Plant Nutr. 62, 212–219.
Cleveland, C.C., et al., 2010. Experimental drought in a tropical rain forest increases soil carbon dioxide losses to the atmosphere. Ecology 91, 2313–2323.
Coby, A.J., et al., 2011. Repeated anaerobic microbial redox cycling of iron. Appl. Environ. Microbiol. 77, 6036–6042.
Druschel, G.K., et al., 2008. Low-oxygen and chemical kinetic constraints on the geochemical niche of neutrophilic iron(II) oxidizing microorganisms. Geochim. Et. Cosmochim. Acta 72, 3358–3370.
Dubinsky, E.A., et al., 2010. Tropical forest soil microbial communities couple iron and carbon biogeochemistry. Ecology 91, 2604–2612.
Emerson, D., et al., 2010. Iron-oxidizing bacteria: an environmental and genomic perspective. Annu. Rev. Microbiol. 64, 561–583.
Fageria, N.K., et al., 2008. Iron toxicity in lowland rice. J. Plant Nutr. 31, 1676–1697.
Fortin, D., Langley, S., 2005. Formation and occurrence of biogenic iron-rich minerals. Earth-Sci. Rev. 72, 1–19.
Gault, A.G., et al., 2011. Microbial and geochemical features suggest iron redox cycling within bacteriogenic iron oxide-rich sediments. Chem. Geol. 281, 41–51.
Ginn, B., et al., 2017. Rapid iron reduction rates are stimulated by high-amplitude redox fluctuations in a tropical forest soil. Environ. Sci. Technol. 51, 3250–3259.
Guelke, M., et al., 2010. Determining the stable Fe isotope signature of plant-available iron in soils. Chem. Geol. 277, 269–280.
Hall, S.J., et al., 2016. Iron addition to soil specifically stabilized lignin. Soil Biol. Biochem. 98, 95–98.
Hall, S.J., Huang, W., 2017. Iron reduction: a mechanism for dynamic cycling of occluded cations in tropical forest soils? Biogeochemistry 136, 91–102.
Hall, S.J., Silver, W.L., 2013. Iron oxidation stimulates organic matter decomposition in humid tropical forest soils. Glob. Change Biol. 19, 2804–2813.
Hall, S.J., Silver, W.L., 2015. Reducing conditions, reactive metals, and their interactions can explain spatial patterns of surface soil carbon in a humid tropical forest. Biogeochemistry 125, 149–165.
Hansen, M., et al., 2014. Flooding-induced N2O emission bursts controlled by pH and nitrate in agricultural soils. Soil Biol. Biochem. 69, 17–24.
Holmgren, G.G.S., 1967. A rapid citrate-dithionite extractable iron procedure. Soil Sci. Soc. Am. J. 31, 210–211.
Hori, T., et al., 2010. Identification of iron-reducing microorganisms in anoxic rice paddy soil by 13C-acetate probing. ISME J. 4, 267–278.
Hou, H., et al., 2012. Seasonal variations of CH4 and N2O emissions in response to water management of paddy fields located in Southeast China. Chemosphere 89, 884–892.
Huang, L.-M., et al., 2018. Variations and controls of iron oxides and isotope compositions during paddy soil evolution over a millennial time scale. Chem. Geol. 476, 340–351.
Huang, W., et al., 2019. Enrichment of lignin-derived carbon in mineral-associated soil organic matter. Environ. Sci. Technol. 53, 7522–7531.
Inubushi, K., et al., 2018. Effect of oxidizing and reducing agents in soil on methane production in Southeast Asian paddies. Soil Sci. Plant Nutr. 64, 84–89.
Jansson, J.K., Hofmockel, K.S., 2020. Soil microbiomes and climate change. Nat. Rev. Microbiol. 18, 35–46.
Kaiser, K., Zech, W., 2000. Dissolved organic matter sorption by mineral constituents of subsoil clay fractions. J. Plant Nutr. Soil Sci. 163, 531–535.
Keiluweit, M., et al., 2017. Anaerobic microsites have an unaccounted role in soil carbon stabilization. Nat. Commun. 8, 1771.
Kettler, T.A., et al., 2001. Simplified method for soil particle-size determination to accompany soil-quality analyses. Soil Sci. Soc. Am. J. 65, 849–852.
Khan, I., et al., 2019. Labile organic matter intensifies phosphorous mobilization in paddy soils by microbial iron (III) reduction. Geoderma 352, 185–196.
Khan, S., et al., 2013. Sewage sludge biochar influence upon rice (Oryza sativa L) yield, metal bioaccumulation and greenhouse gas emissions from acidic paddy soil. Environ. Sci. Technol. 47, 8624–8632.
Kögel-Knabner, I., et al., 2010. Biogeochemistry of paddy soils. Geoderma 157, 1–14.
Kraemer, S.M., 2004. Iron oxide dissolution and solubility in the presence of siderophores. Aquat. Sci. 66, 3–18.
Kwan, W.P., Voelker, B.M., 2002. Decomposition of hydrogen peroxide and organic compounds in the presence of dissolved iron and ferrihydrite. Environ. Sci. Technol. 36, 1467–1476.
Lalonde, K., et al., 2012a. Preservation of organic matter in sediments promoted by iron. Nature 483, 198–200.

Lalonde, K., et al., 2012b. Preservation of organic matter in sediments promoted by iron. Nature 483, 198.
Lehmann, J., Kleber, M., 2015. The contentious nature of soil organic matter. Nature 528, 60–68.
Li, Y., et al., 2012. Are the biogeochemical cycles of carbon, nitrogen, sulfur, and phosphorus driven by the "FeIII–FeII redox wheel" in dynamic redox environments? J. Soils Sediment. 12, 683–693.
Li, Z., Horikawa, Y., 1997. Stability behavior of soil colloidal suspensions in relation to sequential reduction of soils. Soil Sci. Plant Nutr. 43, 911–919.
Liptzin, D., Silver, W.L., 2015. Spatial patterns in oxygen and redox sensitive biogeochemistry in tropical forest soils. Ecosphere 11.
Liu, Y., et al., 2021. Rice paddy soils are a quantitatively important carbon store according to a global synthesis. Commun. Earth Environ. 2, 154.
Lützow, M. v, et al., 2006. Stabilization of organic matter in temperate soils: mechanisms and their relevance under different soil conditions – a review. Eur. J. Soil Sci. 57, 426–445.
McGroddy, M., Silver, W.L., 2000. Variations in belowground carbon storage and soil CO_2 flux rates along a wet tropical climate gradient1. Biotropica 32, 614–624.
McKeague, J.A., 1967. An evaluation of 0.1 M pyrophosphate and pyrophosphate-dithionite in comparison with oxalate as extractants of the accumulation products in podzols and some other soils. Can. J. Soil Sci. 47, 95–99.
McNicol, G., Silver, W.L., 2014. Separate effects of flooding and anaerobiosis on soil greenhouse gas emissions and redox sensitive biogeochemistry. J. Geophys. Res.: Biogeosci. 119, 557–566.
McNicol, G., Silver, W.L., 2015. Non-linear response of carbon dioxide and methane emissions to oxygen availability in a drained histosol. Biogeochemistry 123, 299–306.
Mejia, J., et al., 2016. Influence of oxygen and nitrate on Fe (Hydr)oxide mineral transformation and soil microbial communities during redox cycling. Environ. Sci. Technol. 50, 3580–3588.
Melton, E.D., et al., 2014. The interplay of microbially mediated and abiotic reactions in the biogeochemical Fe cycle. Nat. Rev. Microbiol. 12, 797.
Moorcroft, M.J., et al., 2001. Detection and determination of nitrate and nitrite: a review. Talanta 54, 785–803.
Neubauer, S.C., et al., 2005. Seasonal patterns and plant-mediated controls of subsurface wetland biogeochemistry. Ecology 86, 3334–3344.
Pan, W., et al., 2016. Dissimilatory microbial iron reduction release DOC (dissolved organic carbon) from carbon-ferrihydrite association. Soil Biol. Biochem. 103, 232–240.
Pasakarnis, T., et al., 2015. FeIIaq–FeIIIoxide electron transfer and Fe exchange: effect of organic carbon. Environ. Chem. 12, 52–63.
Peng, Q.-a, et al., 2015. Effects of soluble organic carbon addition on CH4 and CO_2 emissions from paddy soils regulated by iron reduction processes. Soil Res. 53, 316–324.
Riedel, T., et al., 2013. Iron traps terrestrially derived dissolved organic matter at redox interfaces. Proc. Natl. Acad. Sci. 110, 10101–10105.
Schädel, C., et al., 2016. Potential carbon emissions dominated by carbon dioxide from thawed permafrost soils. Nat. Clim. Change 6, 950–953.
Scheiner, D., 1976. Determination of ammonia and Kjeldahl nitrogen by indophenol method. Water Res. 10, 31–36.
Schwertmann, U., 1973. Use of oxalate for fe extraction from soils. Can. J. Soil Sci. 53, 244–246.
Sodano, M., et al., 2017. Dissolved organic carbon retention by coprecipitation during the oxidation of ferrous iron. Geoderma 307, 19–29.
Spohn, M., Giani, L., 2010. Water-stable aggregates, glomalin-related soil protein, and carbohydrates in a chronosequence of sandy hydromorphic soils. Soil Biol. Biochem. 42, 1505–1511.
Sun, Z., et al., 2019. Effects of iron(III) reduction on organic carbon decomposition in two paddy soils under flooding conditions. Environ. Sci. Pollut. Res. 26, 12481–12490.
Tamura, H., et al., 1974. Spectrophotometric determination of iron(II) with 1,10-phenanthroline in presence of large amounts of iron(III). Talanta 21, 314–318.
ThomasArrigo, L.K., et al., 2022. Mineral characterization and composition of Fe-rich flocs from wetlands of Iceland: Implications for Fe, C and trace element export. Sci. Total Environ. 816, 151567.
Thompson, A., et al., 2006. Iron-oxide crystallinity increases during soil redox oscillations. Geochim. Et. Cosmochim. Acta 70, 1710–1727.
Thompson, A., et al., 2011. Iron solid-phase differentiation along a redox gradient in basaltic soils. Geochim. Et. Cosmochim. Acta 75, 119–133.
Wagai, R., Mayer, L.M., 2007. Sorptive stabilization of organic matter in soils by hydrous iron oxides. Geochim. Et. Cosmochim. Acta 71, 25–35.
Wang, M.L., et al., 2016. Iron oxidation affects nitrous oxide emissions via donating electrons to denitrification in paddy soils. Geoderma 271, 173–180.
Wang, P., et al., 2019. The role of iron oxides in the preservation of soil organic matter under long-term fertilization. J. Soils Sediment. 19, 588–598.
Wang, Y.S., Wang, Y.H., 2003. Quick measurement of CH4, CO_2 and N2O emissions from a short-plant ecosystem. Adv. Atmos. Sci. 20, 842–844.
Weber, K.A., et al., 2006. Microorganisms pumping iron: anaerobic microbial iron oxidation and reduction. Nat. Rev. Microbiol. 4, 752–764.
Wen, Y., et al., 2019a. Impact of agricultural fertilization practices on organo-mineral associations in four long-term field experiments: Implications for soil C sequestration. Sci. Total Environ. 651, 591–600.
Wen, Y., et al., 2019b. Is the 'enzyme latch' or 'iron gate' the key to protecting soil organic carbon in peatlands? Geoderma 349, 107–113.
Xu, J.-X., et al., 2019. Fate of labile organic carbon in paddy soil is regulated by microbial ferric iron reduction. Environ. Sci. Technol. 53, 8533–8542.
Yi, L., et al., 2022. Differential contributions of electron donors to denitrification in the flooding-drying process of a paddy soil. Appl. Soil Ecol. 177, 104527.
Zhao, Q., et al., 2016. Iron-bound organic carbon in forest soils: quantification and characterization. Biogeosciences 13, 4777–4788.
Zhao, Q., et al., 2017. Coupled dynamics of iron and iron-bound organic carbon in forest soils during anaerobic reduction. Chem. Geol. 464, 118–126.